Assessing the impact of climate change on water resources, crop production and land degradation in a semi-arid river basin

Ammar Rafiei Emam, Martin Kappas and Seyed Zeynalabedin Hosseini

ABSTRACT

The semi-arid regions of Iran have experienced severe water resources stress due to natural (e.g., drought) and anthropogenic (e.g., depletion of water in various sectors) factors. Assessing the impact of climate change on water resources and crop production could significantly help toward better water management and hence prevention of land degradation in this area. A hydrological model of the Razan–Ghahavand basin was used as a representative case study of a semi-arid region of Iran. Future climate scenarios in the mid-21st century were generated from four global circulation models (GCMs) with three scenarios under the fourth assessment report of Intergovernmental Panel on Climate Change emission projections. The GCMs have been downscaled based on observed data at 10 climate stations across the basin. The results showed that for the basin as a whole, the mean annual precipitation is likely to decrease while the maximum temperature increases. The changes in these two climate variables resulted in substantial reduction in groundwater recharge as the main source of water supply in this area. Furthermore, soil water content was decreased which resulted in the reduction of crop yield in rain-fed areas. Indeed, the risk of drought in the south and flooding in the north was high.

Key words | climate change, food security, semi-arid area, water resources

Ammar Rafiei Emam (corresponding author)
Department of Cartography,
GIS and Remote Sensing,
Georg-August-University of Göttingen,
Goldschmidtstr. 5,
37077 Göttingen,
Germany
E-mail: *rafiei99@gmail.com*

Ammar Rafiei Emam
Martin Kappas
Seyed Zeynalabedin Hosseini
Department of Natural Resources and Desert Studies,
University of Yazd,
Yazd,
Iran

INTRODUCTION

Semi-arid regions suffer from shortage of water. Climate variation alongside anthropogenic factors such as population growth, land use changes, and overuse of water resources especially for irrigation, are significant concerns. Climate change and its impact on water resources are a further challenge in the sensitive and fragile ecosystems such as the semi-arid regions of Iran. The availability of water resources, crop production and the process of land degradation should be future considerations in this area in order to build up a sustainable ecosystem and to improve food security. However, the uncertainty of global circulation models (GCMs) may lead to different results in the same area (Singh & Bengtsson 2005; WWF 2010; Gosain *et al.* 2011). Therefore, we developed an ensemble of GCMs to predict the water availability and also the capacity of crop production in the semi-arid region of Iran.

Hijioka *et al.* (2014) in IPCC-AR5 mentioned that increasing water demand and mismanagement of water resources give rise to water scarcity as a major challenge for most regions in Asia. According to IPCC (2007a), climate change has a pernicious effect on water resources and freshwater availability in most of the regions of the world. It can also have a significant impact on the hydrological cycle (Piao *et al.* 2009; Wu *et al.* 2012). IPCC (2013) in their AR5 report revealed that human influence in global warming and changing of water cycle has grown since the fourth assessment report (AR4). The quantum of damages, however, can differ from one place to another. The variation of precipitation and temperature characteristics can lead to land degradation especially in fragile arid and semi-arid ecosystems (Meadows & Hoffman 2003). The variation of

doi: 10.2166/nh.2015.143

intensity and variability of precipitation leads to increasing risks of droughts and floods in most regions. Furthermore, alteration in floods and droughts and a rise in water temperature are changing the water quality (IPCC 2007b). IPCC (2014) reported that drought frequency would likely rise in the current dry regions by the end of the 21st century. Shifts in precipitation and temperature result in variations of groundwater recharge and also cause water table fluctuations (Changnon *et al.* 1988; Zektser & Loaiciga 1993). In addition, changes in groundwater recharge can have an influence on evapotranspiration (ET), groundwater flow direction, groundwater level and surface water–groundwater interaction (Ali *et al.* 2012).

Land use changes (particularly urbanization) could alter the hydrological response of an area by changing the amount of rainwater that goes into surface discharge and groundwater recharge (Baker & Miller 2013). However, the impact of land use/land cover change varies with the climatic conditions (Kim *et al.* 2013). Human activities and climate variability can influence the hydrological processes (e.g., annual runoff, stream flow) especially in semi-arid regions (Zhan *et al.* 2013; Xu *et al.* 2013). Zhou *et al.* (2013) revealed that surface runoff and base flow are very sensitive to urbanization, whereas ET and annual streamflow are less sensitive. Many previous studies identified a combined effect of climate and land use change on water components (e.g., surface runoff) (Tu 2009; Tong *et al.* 2012; Kim *et al.* 2013).

Food-producing capacity and livestock production can be significantly affected by climate change for years to come. While some areas may experience a decrease in crop production, others are likely to increase. CO_2 concentration and temperature are two important factors affecting crop production. While increasing CO_2 concentration as the main driver of climate change could raise production of some crops (e.g., wheat), the changing climate, in general, is likely to have a negative effect on the length and quality of the growing season. In addition, having a higher intensity of droughts and floods could have countless consequences for crop production. On the other hand, a temperature increase of a few degrees is expected to generally raise crop production in temperate areas; however, greater warming may decrease crop yields (Adams *et al.* 1998; Raleigh & Urdal 2007).

Assessing the impact of climate change on hydrological processes can be used with various hydrological models (e.g., Rosenberg *et al.* 1999; Kirshen 2002). For instance, the hydrologic unit model of the USA was used to assess the impact of global warming on the hydrology of the Ogallala area in the United States, where the comparison of different GCMs shows an influence on the reduction of groundwater recharge (Rosenberg *et al.* 1999). Eckhardt & Ulbrich (2003) used a revised version of soil and water assessment tools (SWAT) to investigate the impact of climate change on groundwater recharge and stream flow in a central European low mountain range. The results of their studies show little effect of climate change on mean annual groundwater recharge and stream flow. In this research, we used the SWAT eco-hydrologic model (Arnold *et al.* 1998) to study the impact of climate change on water resources and crop productions. Various investigations show the benefit of SWAT to assess the impact of climate change (Fontaine *et al.* 2001; Young *et al.* 2009; Faramarzi *et al.* 2013).

As water resources in Iran become scarcer due to recurrent droughts and rising demand, accurate knowledge of the available resources in the future is mandatory for successful management. The fresh water availability in the semi-arid region of Razan–Ghahavand has experienced severe reduction due to increasing demand for sanitation, drinking water, manufacturing and agriculture. All of these factors trigger the expansion of land degradation in this area. To improve water resource management, water use efficiency, sustainability of agriculture and land management to combat degradation in the future, precise knowledge of water resources is needed. There is a close relationship between water resources, industry, agriculture and urban dynamics in this area. Therefore, it is essential to study the climate change impact on hydrology and water resources.

The main objective of this research is to investigate the impact of climate change on water resources' components such as groundwater recharge, soil water content, surface runoff and actual evapotranspiration (AET) for 2046–2065. The effect of land use change (e.g., urbanization) on surface runoff, estimation of crop yields and an analysis of future land degradation are the other objectives of this research. We used the ensemble of four global climate models to quantify the impact of climate change on water resources and crop production in the mid-21st century.

MATERIALS AND METHODS

Study area

The study area called Razan–Ghahavand is located in the central drainage basin of Iran. The area is approximately 3,100 km^2. The range of the highest and lowest elevation inside the watershed is roughly 1,265 m. A variety of species has evolved from the highest to the lowest elevation following this gradient. The climate of this region is semi-arid with an annual average temperature around 11 °C and annual average precipitation of about 295 mm. The main river in the watershed, called Gharehchay, enters the watershed from the west whereas the watershed's outlet is controlled by the Omarabad hydrometric station in the eastern part of the watershed. In addition, two other streams, Sirab Khomigan and Zehtaran, respectively, join the main river from the northern part of the basin. In Table 1, the watershed area covered by the single hydrometric stations and their sub-basins is shown. According to the land use map, about 52% of the area is grazing land covered by species that occur in different numbers and with a varying capacity for livestock rearing. Irrigation farming covers 26% and rain-fed cultivation covers 5% of the watershed area.

Owing to traditional irrigation methods and water conveyancing systems, the efficiency of water use is only 35% and substantial amounts of water are lost (Abrishamchi & Tajrishi 2005). Figure 1 shows the location of the study area inside Iran including all available hydrometric and meteorological stations. There are various features of land degradation phenomena in this basin. In the south of the area, rangelands have deteriorated. In the west of the basin, the groundwater level has decreased and land subsidence has occurred. In the eastern part, arable lands are salinized (Figure 2).

The SWAT simulator, model setup, calibration and uncertainty analysis

We used SWAT (Arnold *et al.* 1998) to assess the influence of climate change on water resources and crop production. SWAT is a hydrological model to study the quality and quantity of surface and ground water resources and predict the impact of land use, land management and climate change on water resources. It is a physical, distributed and continuous time model that operates on a daily time assessment. The main components of SWAT include hydrology, climate, nutrient cycle, sediment movement, crop growth and agricultural management. Hydrological processes in SWAT simulate surface runoff, potential evapotranspiration (PET), percolation, lateral subsurface flow, groundwater flow to streams from shallow aquifers, snowmelt, transmission losses from streams, and water storage and losses from ponds (Neitsch *et al.* 2011). Hydrological response units (HRUs) including homogenous land use, soil and slope characteristics are the units of water balance calculations. The water in each HRU is stored in four storage volumes including snow, soil profile (0–2 m), shallow aquifer (2–20 m) and deep aquifer (>20 m).

Basic input data include climate data, soil information, a digital elevation map, a river map, a land use classification plus crop and agricultural management data. All data are needed to set up a SWAT hydrologic model run. Climate data consist of daily precipitation, daily minimum and maximum temperature and daily solar radiation obtained from the weather service of the Iranian meteorological organization from 1977 to 2008. As the watershed is not located at the headwater of a particular basin, the inlet was defined for catchment. In other words, inlet is defined as estimating the amount of water entering the basin. The surface runoff inside the catchment is estimated by the SCS curve number method based on daily precipitation, soil hydrologic

Table 1 | Sub-basins affected with flow in each station including with rate of discharge

No.	Station name	Location (in the sub-basin)	Sub-basins	Area (km^2)	Discharge (m^3 s^{-1})
I	Sirab–Khomigan	14	1, 2, 3, 4, 5, 6, 12, 13, 14	255	0.33
II	Zehtaran	41	23, 26, 27, 28, 29, 32, 33, 34, 37, 38, 41	420	0.66
III	Omarabad	71	All sub-basins	3,100	6.68

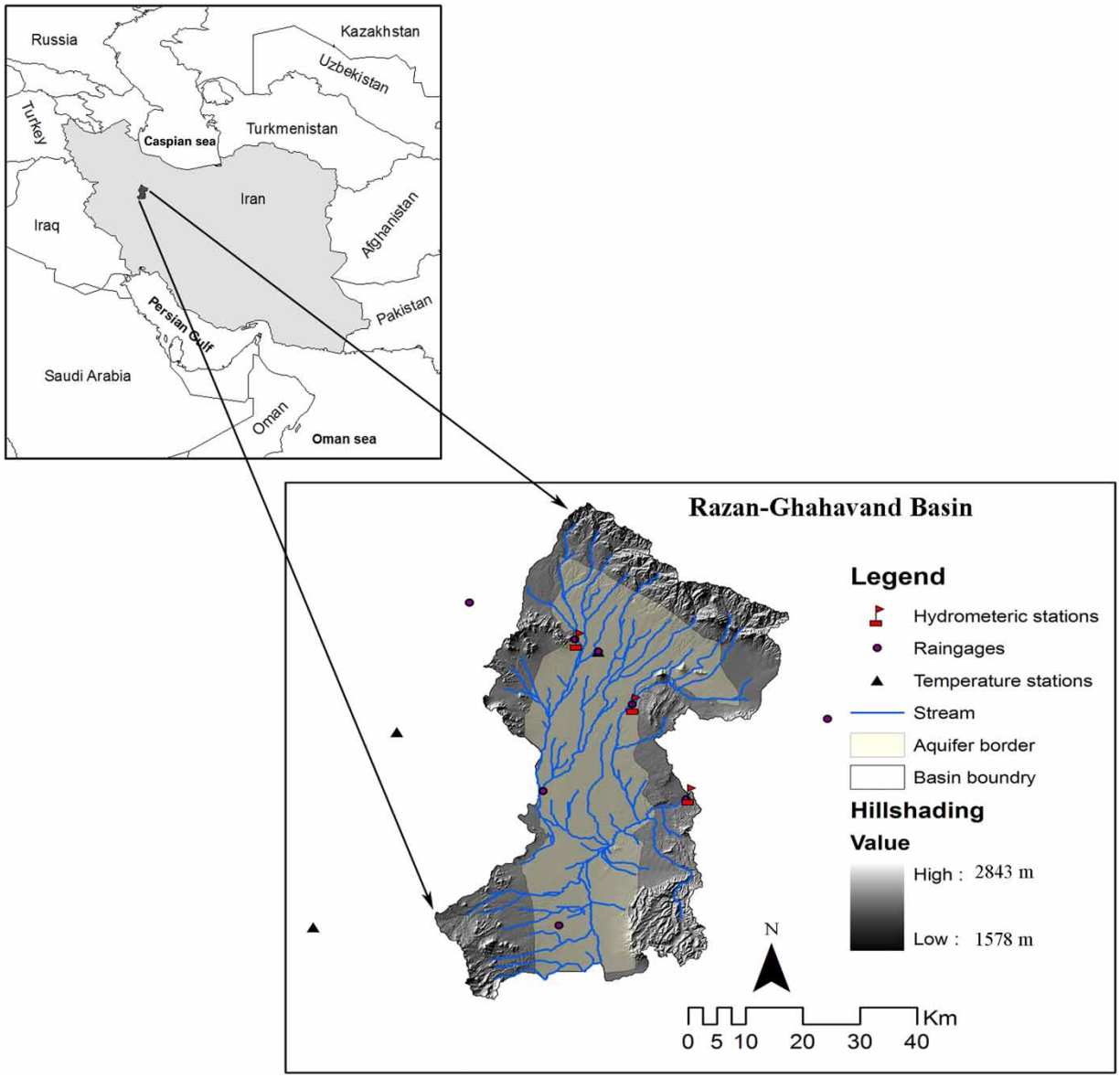

Figure 1 | Region of Razan–Ghahavand watershed showing the hypsometric map, distribution of river and streams, hydrometric and climatic stations (e.g., rain gage and synoptic).

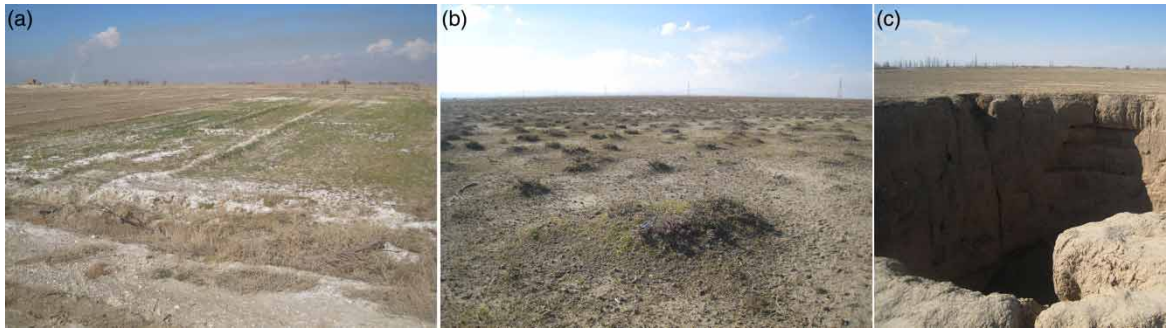

Figure 2 | Some features of land degradation in the area (e.g., soil salinization in arable lands, rangeland degradation and land subsidence).

groups, antecedent soil moisture plus different mapped land use. To adapt the model to the specific study area's conditions, the curve number (CN) is modified in relation to changing slope factors. To define the impact of elevation difference on the model, elevation bands are defined for sub-basins, an elevation difference of more than 100 m using a specific temperature lapse rate [°C/km] and precipitation lapse rate [mm H_2O/km] value. To route water through the channel network, a variable storage routing method is chosen. The crop growth is simulated based on the Erosion-Productivity Impact Calculator (EPIC) method (Williams *et al.* 1984) by determining leaf area development (LAI), light interception and radiation use efficiency. Winter wheat is selected as the dominant crop in agricultural lands both for rain-fed and irrigated lands. Schedule planning (e.g., time of planting, irrigation, fertilization, harvesting) was defined both for irrigated and rain-fed farmlands according to real information obtained from farmers and the Hamedan Agricultural Organization. Irrigation application is simulated based on an auto-irrigation routine, because it is difficult to know the volume and specific time of irrigation by farmers during simulation periods. Auto-irrigate triggers irrigation events based on water stress threshold. To estimate PET the Hargreaves method (Hargreaves & Samani 1985) is used. AET is obtained based on the Ritchie methodology (Ritchie 1972).

Several researchers have reported an uncertainty quantification of the hydrological models (Jin *et al.* 2010; Li *et al.* 2010, 2013). Li & Xu (2014) used Bayesian and generalized likelihood uncertainty estimation methods to estimate the uncertainty of a hydrological model. Abbaspour (2007) developed a SUFI-2 (sequential uncertainty fitting) method to analyse the uncertainty of the hydrological models.

After setting up a SWAT model run, a SUFI-2 algorithm is used for uncertainty analysis and to calibrate the model based on the monthly river discharge and yearly crop yield. The SUFI-2 represents all modeling sources of uncertainties such as input data, conceptual model and parameter selections. The uncertainties are mapped based on the parameter ranges. The algorithm tries to bracket most of the measured data within the 95% prediction uncertainty band (95PPU) which is calculated at 2.5 and 97.5% of the cumulative distribution of an output variable obtained through Latin hypercube sampling. To quantify the goodness of calibration and uncertainty performance two indices (*P*-factor and *R*-factor) are used. The *P*-factor is the percentage of data bracketed by the 95PPU band and the *R*-factor is the average width of the 95PPU band divided by the standard deviation (SD) of the measured data. To compare the measured and simulated monthly discharge and annual crop yield, Nash–Sutcliffe (NS) and root mean square error (RMSE) objective functions are used, respectively. In this research, we used a previously calibrated SWAT model of the Razan–Ghahavand river system. A detailed description about calibration, validation, uncertainty and sensitivity analysis is presented by Rafiei Emam *et al.* (2015a).

Climate change model

An increasing CO_2 concentration will have a severe effect on vegetation, especially on leaf area index development and stomata conductance (Wand *et al.* 1999) and, additionally, it can lead to changes in ET resulting in change to other water components.

The impact of climate change on water resources and crop production was assessed by developing a set of GCMs parameterized based on three IPCC-AR4 emission scenarios (A1B, B1 and A2) in the middle of the 21st century (2046–2065) defined by the Intergovernmental Panel on Climate Change (IPCC 2007a). The approved new set of scenarios is described in the IPCC Special Report on Emission Scenarios (SRES). Four different narrative storylines were developed to consistently describe the relationships between the forces driving emissions and their evolution and to add context to the scenario quantification. The resulting scenarios cover a wide range of the main demographic, economic and technological driving forces of future greenhouse gas and sulfur emissions. The B1 storyline and scenario family describes a convergent world with the same global population, that peaks in mid-century and declines thereafter, as in the A1 storyline, but with rapid change in economic structures toward a service and information economy, with reductions in material intensity and the introduction of clean and resource-efficient technologies. The emphasis is on global solutions to economic, social and environmental sustainability, including improved equity, but without additional climate initiatives. The three

A1 groups are distinguished by their technological emphasis: fossil intensive (A1FI), non-fossil energy sources (A1 T), or a balance across all sources (A1B) (where balance is defined as not relying too heavily on one particular energy source, on the assumption that similar improvement rates apply to all energy supply and end-use technologies). The A2 storyline and scenario family describes a very heterogeneous world. The underlying theme is self-reliance and preservation of local identities. Fertility patterns across regions converge very slowly, which results in a continuously increasing population. Economic development is primarily regionally oriented and per capita economic growth and technologies change in a more fragmented and slower way than in other storylines.

Spatial resolution of GCM output is coarse (i.e., low resolution) therefore we applied a downscaling program (LARS-WG) developed by Semenov & Stratonovitch (2010) in order to generate fine resolution climate data to use the output in the hydrological model. LARS-WG is a model simulating time-series of daily weather at a single site. It utilizes semi-empirical distribution to obtain statistical parameters such as length of wet and dry periods, daily precipitation, daily minimum and maximum temperature and daily solar radiation based on daily observed climate data at local stations of the catchment. For the minimum and maximum temperature, auto- and cross-correlation calculated monthly were used by semi-empirical distribution calculation. For solar radiation, semi-empirical distributions with equal interval sizes are used. LARS-WG has been successfully tested in several case studies with diverse climate types (e.g., Lawless & Semenov 2005; Zarghami *et al.* 2011; Sunyer *et al.* 2012). The new version of LARS-WG includes the data for different GCM models. A number of statistical tests such as *t*-test, *F*-test and chi-squared test were implemented by LARS-WG in order to verify the results of the simulation by comparing the synthetic data with the observed data.

Our climate model provided downscaled output from four GCMs (CCSM3, CSIRO-MK3, MPEH5 and HADGEM). We developed a multi-model ensemble from these GCMs. An ensemble of climate models exhibits more reliable representation of regional and local uncertainties than results from individual GCMs by decreasing the biases from single models (Abbaspour *et al.* 2009; Gaiser *et al.* 2011; Wu *et al.* 2012). After downscaling GCM data, the daily climate data were put into the SWAT calibrated eco-hydrologic model to simulate the future impacts on water components. Parameter ranges in the hydrologic model represent the uncertainty of the model run. According to the calibrated model, 69 sets of eco-hydrologic parameters were used to capture the uncertainty of the model (e.g., CN2, alpha_bf). The model was then run for a baseline scenario (1998–2008) and future climate scenarios (2046–2065). The CO_2 concentration was defined as 492, 541 and 545 ppm for the selected climate scenarios B1, A1B and A2, respectively (Semenov & Stratonovitch 2010).

Land use change (urbanization)

We estimated the impact of urbanization on surface runoff in our study area. To examine the land use change, two series of satellite images in 1989 and 2009 were used. The land use of 2009 was adopted for the SWAT model. Based on changes in land use during 20 years (1989–2009), future land use (2050) was predicted. Moreover, population and its growth rates were used as a driver in land use prediction (2046–2065).

RESULTS AND DISCUSSION

We used a previously calibrated SWAT model of the Razan–Ghahavand area (Rafiei Emam *et al.* 2015b). The model's performance was satisfactory for both calibration and validation periods. The NS model efficiency ranged from 0.53 to 0.63 for calibration and from 0.42 to 0.72 for validation for river discharge. Santhi *et al.* (2001) and Moriasi *et al.* (2007) mentioned that the model performances can be evaluated as satisfactory if NS and R^2 are greater than 0.5. The RMSE for crop (rain-fed wheat) calibration and validation was 0.07 and 0.25 ton ha^{-1}, respectively. In irrigated wheat the RMSE was estimated as 0.19 and 0.691 ton ha^{-1}, respectively, showing a good performance of the model. Generally, a good calibration with crop yield leads to a good calibration of ET, adding more confidence to simulation of soil moisture and groundwater recharge. Figure 3 shows the calibration and validation performance of the SWAT model based on the river discharge at the Omarabad

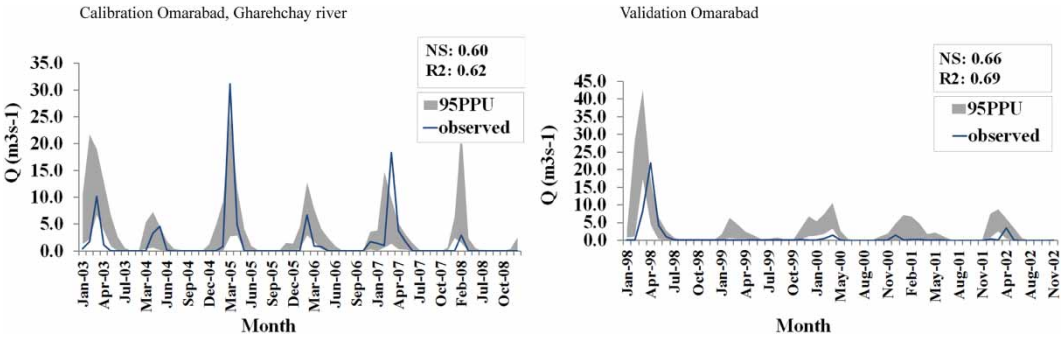

Figure 3 | Results of SWAT calibration–validation for one selected hydrometric station.

station. More details on calibration, uncertainty analysis and model results can be found in Rafiei Emam *et al.* (2015a, b).

Downscaling results

To assess the reliability of the downscaling result, the mean and SD of observed and generated values of rainfall and temperature from 1983 to 2009 were calculated for the Ghahavand station in the south of the area (Figure 4(a) and 4(b)). The results showed that the simulated and observed mean and SD of temperature and rainfall are close together which indicates the high reliability of the simulation.

Impact of climate change on precipitation and temperature

The results revealed that the annual precipitation decreased between 8 and 35 mm in different scenarios. The same result of reduced annual precipitation in the period of 2046–2065 was reported by Zarghami *et al.* (2011) in the northwest of Iran. Figure 5 compares the prediction of monthly mean precipitation for the period from 2046 to 2065 using the GCMs and base line in the study area. The three scenarios have a tendency to raise monthly mean precipitation at the end of autumn but are less pronounced during spring and summer. This shortfall in precipitation, especially in spring, will increase the water stress. The water stress has an effect on crop production and rangeland species especially in the south of the watershed. The monthly mean precipitation will be decreased in scenario A1B more than A2 and B1.

The spatial distribution of annual precipitation in the historic period (1998–2008), per cent changes of precipitation based on the future (2046–2065) and historic data are shown in Figure 6(a)–6(d). The precipitation will decrease in the south, east and northeast of the watershed up to 18% for scenario A1B. In scenarios A2, precipitation will decrease from 5 to 10% in the south of the watershed while in scenario B1, precipitation will decrease only up to 5% for the duration of the period 2046–2065. The spatial

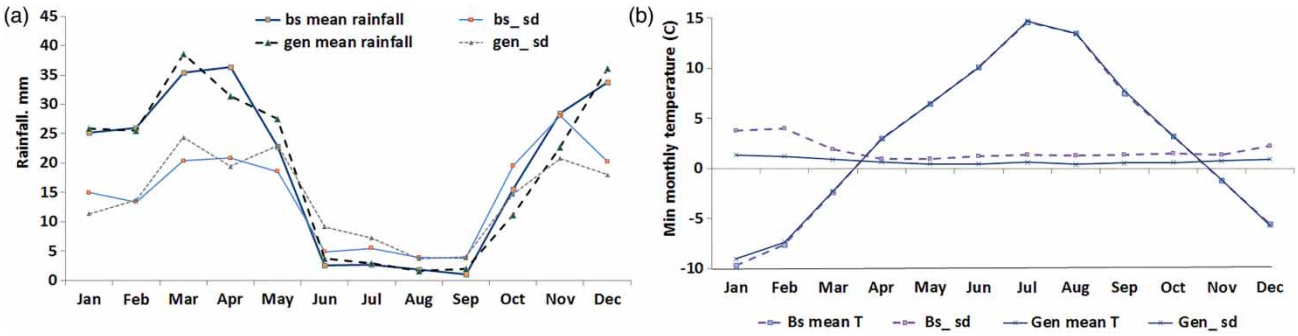

Figure 4 | Comparison of the observed and generated mean and SD of (a) monthly rainfall and (b) minimum temperatures at the Ghahavand station (1983–2009). BS: base line, gen: generated, SD: standard deviation.

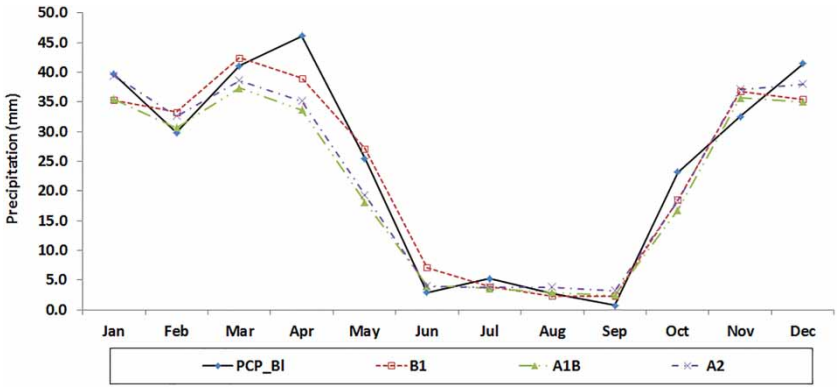

Figure 5 | Mean monthly precipitation in baseline (1997–2008) and future (2046–2065) in three different emission scenarios according to the ensemble multi-models.

patterns show that in the west of the study area the precipitation is rising up to 27% in scenario B1.

As precipitation is already low in the southern lowlands of the watershed, the decline of precipitation may have a significant influence on increasing drought in the future. Hence, crop production and rangeland productivity in this area will be at a lower level which may lead to more land degradation and desertification. Rangelands in the northern and southern parts of the watershed are directly affected by precipitation and soil moisture distribution. The rangelands in the southern portion of the area are more sensitive than in the northern part due to lower precipitation and hence lower soil moisture.

Figure 7 shows the absolute alteration of the surface temperature for three different emission scenarios (A1B, A2 and B1) at Dargazin station located in the north of the watershed. The figure reveals that the average temperature will rise by approximately 2.3 °C. In total, the emission scenarios have a tendency to raise the maximum (T_{max}) and minimum (T_{min}) temperatures throughout the year. The highest increase was found with the A2 scenario for T_{min} (about 58% change), whereas the lowest increase occurred with the B1 scenario for T_{max} (change of 5.2%).

Figure 6(e)–6(h) show historic patterns of the average maximum temperature (Figure 6(e)) and anomalies of the absolute difference between the maximum temperature prediction of the three scenarios and the average over the future (2046–2065) and historic (1998–2008) period. The results show the changes of maximum temperature in A1B and A2 are more than the B1 emission scenario. In scenarios A1B and A2, most of the north and central watershed experience an increase of about 2 °C in temperature (in scenario B1 about 1 °C) while in the south of the watershed the increase is mostly about 2.5 °C (in B1 scenario about 1.5 °C).

The diurnal temperature range is calculated as the difference between maximum and minimum temperature. For the historic period it is between 14 and 16.5 °C over the watershed area. This difference in the southern area is more than the central and the northern basin. However, the diurnal temperature will decrease in the north and central part of the watershed while it will increase in the south of the watershed during 2046–2065. Hence, the minimum temperature increase is stronger in the north and central part of watershed and lower in most parts of the southern water catchment.

Impact of climate change on water balance components

ET varies considerably across the area due to soil and land cover variations. The annual actual ET varies from 233 to 415 mm with the highest ET in the northern part and lowest in the southern part of the watershed (Figure 6(i)). Approximately 294 mm of the water budget is lost by annual ET, which reveals that ET has the largest portion of the watershed's overall water budget. The percentage difference calculated between ET based on the emission scenarios and the baseline scenario shows that in most parts of the watershed the ET will decrease by up to 17%. However, an increase of ET is seen in the west of the watershed throughout all scenarios (Figure 6(j) and 6(k)). The B1 scenario indicated an increase in ET in the north and central

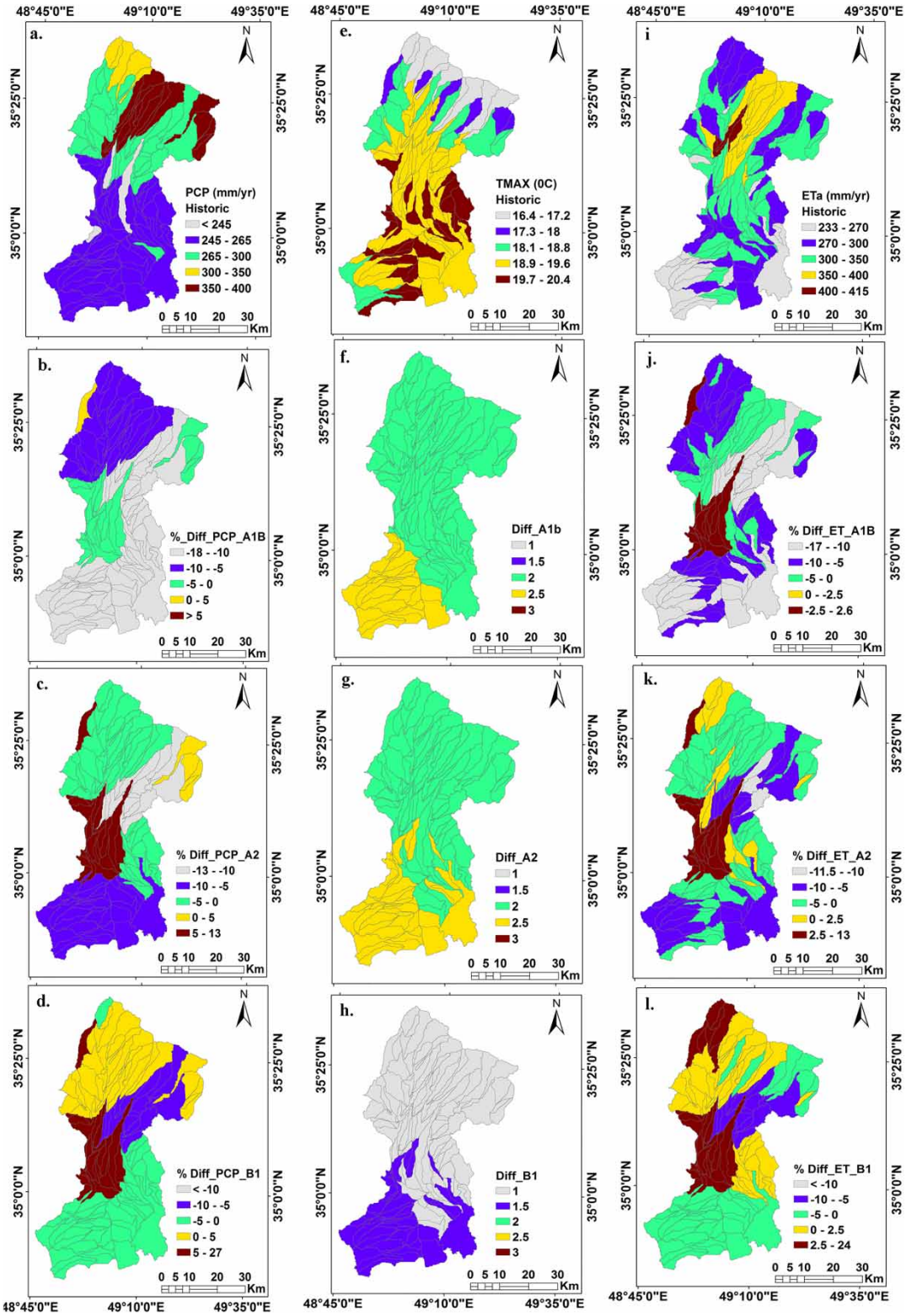

Figure 6 | Spatial pattern of average annual precipitation (a), maximum temperature (e) and AET (i) for the historic period (1998–2008). Percentage difference calculated of precipitation based on future and historic data (b)–(d), % difference maximum temperature (f)–(h) and the pattern of % difference calculated of ET based on future and historic data (j)–(l).

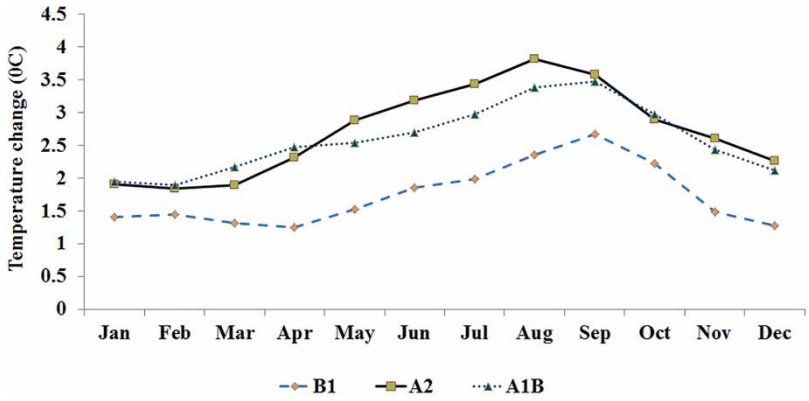

Figure 7 | The absolute surface temperature changes (°C) in north of study area in GCM period with respect to the baseline period for three different emission scenarios.

part of the watershed while scenario A1B illustrated a further decrease in ET.

Groundwater recharge is affected not only by hydrological processes, but also by physical characteristics of the land surface and soil types. The average annual groundwater recharge rate is approximately 5 mm/yr. The groundwater recharge rate responds not only to variation in land use but also to variation of hydraulic soil characteristics and variations in climatic conditions across the watershed. On the other hand, the area is a semi-arid region with low precipitation and high temperature, therefore most of the precipitation will not infiltrate deep into the soil due to high ET. The northern part of the watershed has significantly higher recharge rates than the southern part. The areas with high groundwater recharge may illustrate regions where the underlying aquifers are facing higher contamination vulnerability. This may have a considerable impact on land use planning, where land is being converted into residential areas and/or industrial regions (Jyrkama & Sykes 2006). The groundwater recharge varies significantly over time. In summer, the monthly recharge rate is lower than in other months of the year due to high temperatures and low precipitation. Also, there is no return flow from irrigation in the summer. The results also show that the increase in groundwater recharge in B1 scenario in the west of the basin is much greater than in other scenarios. In scenario A1B, the groundwater recharge shows a greater decrease in the north of the area than in other scenarios (Figure 8(a)–8(d)).

Figure 8(e)–8(h) show the annual spatial pattern of surface runoff in the study area. The northeast and the southwest of the watershed have significantly higher surface runoff due to the existence of low permeability soils. In scenario B1, the surface runoff rate is much higher than in other scenarios especially in the north, center and southwest of the watershed; the increase of surface runoff rises up to 65% in these regions. In the southeast, and some parts of the north of the watershed, the surface runoff decreased to 56%. However, in mountainous areas of the northern portion of the basin the runoff will increase.

The historical data show a soil moisture rate varying from 10 mm in the southwest to 80 mm in the northern portion of the watershed. According to the emission scenarios, soil moisture in the northern and southern portions of the watershed has significantly decreased whereas the central and western part of the area showed an increase of water content. The A1B scenario shows the highest decrease in soil moisture compared to the other scenarios (Figure 8(i)–8(l)).

Land use change scenario

Land use change monitoring indicates that urban or built-up land expanded by about 100% in Razan–Ghahavand during the 1989–2009 periods. The urban land was increased mostly due to the contraction of croplands. Based on this information and according to the mean annual population growth rate in the area reported by the Statistical Center of Iran (2011) of 2.63% during 1986–2006, we assumed the urban or built-up growth is about 190% during the 2046–2065 period. The results indicated that the average annual runoff volume increased by more than 60% from 2045 to 2064 due to

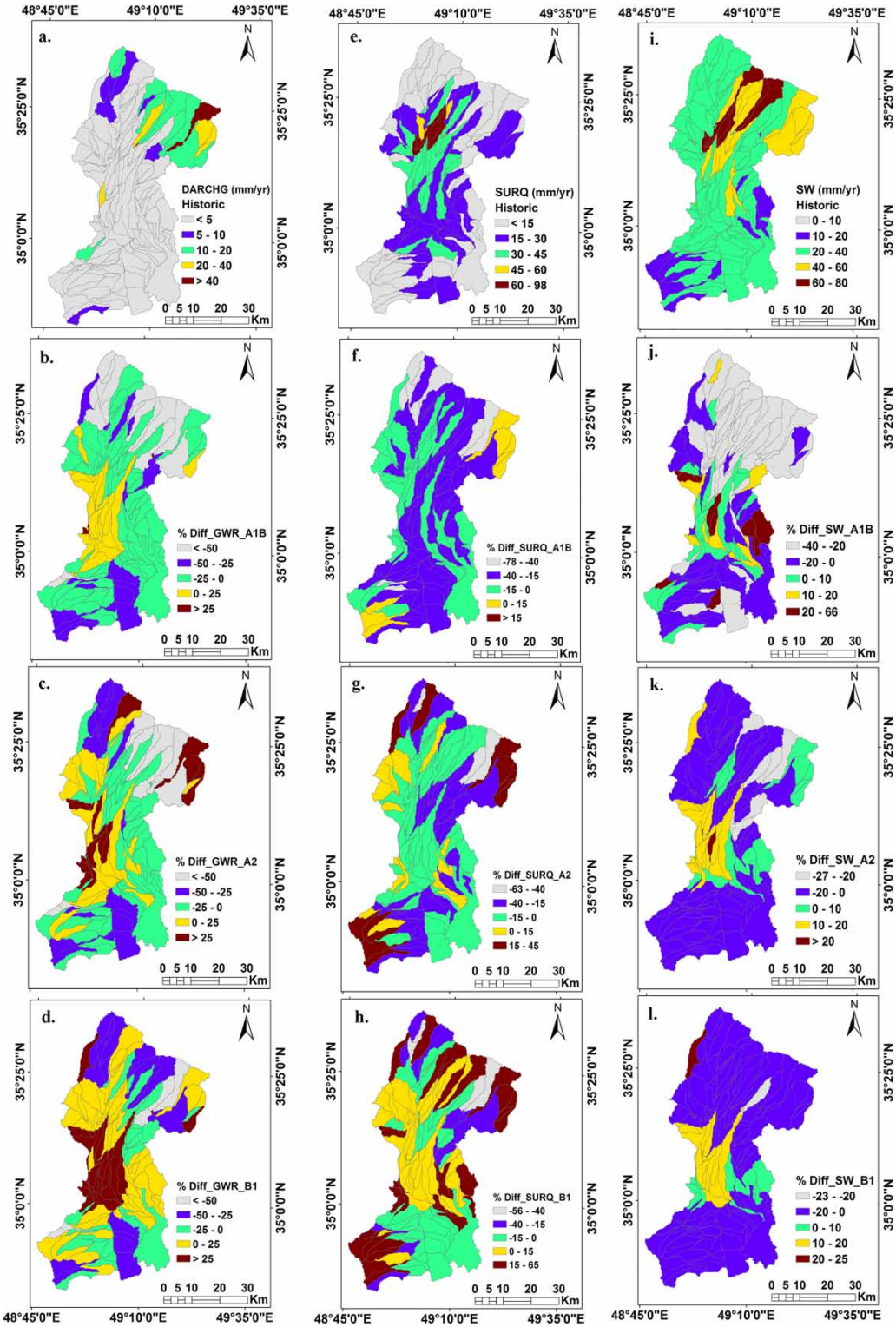

Figure 8 | Spatial pattern of deep aquifer recharge, surface runoff and soil water content in historical (1998–2008) and future (2046–2065) periods. The pattern of deep aquifer recharge (a) and % difference calculated of DARCH based on future and historic data (b)–(d). The distribution of average annual surface runoff (e) and % difference calculated of SURQ based on future and historic data (f)–(h). The spatial pattern of soil water content (i) and % difference calculated of SW based on future and historic data (j)–(l).

urbanization. The increase of surface runoff by urbanization has already been mentioned in other studies (Weng 2001).

Impact of climate change on crop production

Figure 9 depicts anomaly graphs of irrigated and rain-fed wheat yield in the future. The results of the ensemble model show the increase of production in irrigated areas; however, in rain-fed areas the production decreased. The reasons for rising wheat yield in irrigated areas are increasing CO_2 concentration and rising temperature, especially minimum temperature, while the cereals suffered from temperature stress during the historical period (1998–2008). In general, heat stress decreased in all GCM scenarios in comparison with the base line both for irrigated and rain-fed lands (Figure 10). Within the watershed, the heat stress in the south of the region is predicted as 26% less than in the northern part of the plain, which is due to the mean monthly temperature in the south being higher than in the north. The reason for the decreasing rain-fed yield, especially in A1B scenario, is due to decreasing precipitation (−10%) resulting in a decline of soil moisture (−13%). The analysis of water stress shows that it will increase in the future in all scenarios in rain-fed areas as a result of a decrease in predicted rain-fed yield. In irrigated lands, water stress does not change significantly and M95PPU recorded around 75 days stress (Figure 11). The analysis of monthly water stress shows an increase from April to June (both for irrigated and rain-fed lands) which has a pernicious effect on crop production (e.g., Figure 12 revealed the anomaly graph of water stress in the A1B scenario both for irrigated and rain-fed land).

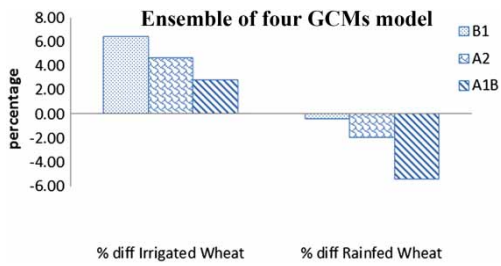

Figure 9 | Anomaly graph of irrigated and rain-fed wheat yield in the GCM scenarios.

Land degradation and water table

There are various land degradation phenomena in the study area. The evidence of these land degradations are salinization in the east and center, rangeland degradation in the south and subsidence in the west of the watershed. Land

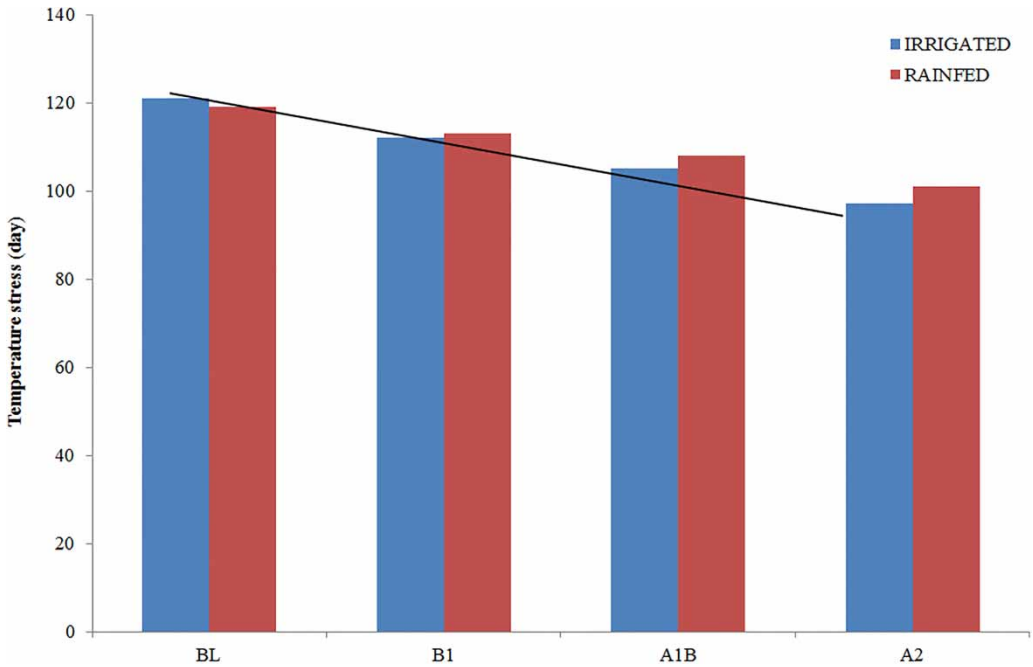

Figure 10 | Temperature stress during growing season for rain-fed and irrigated lands.

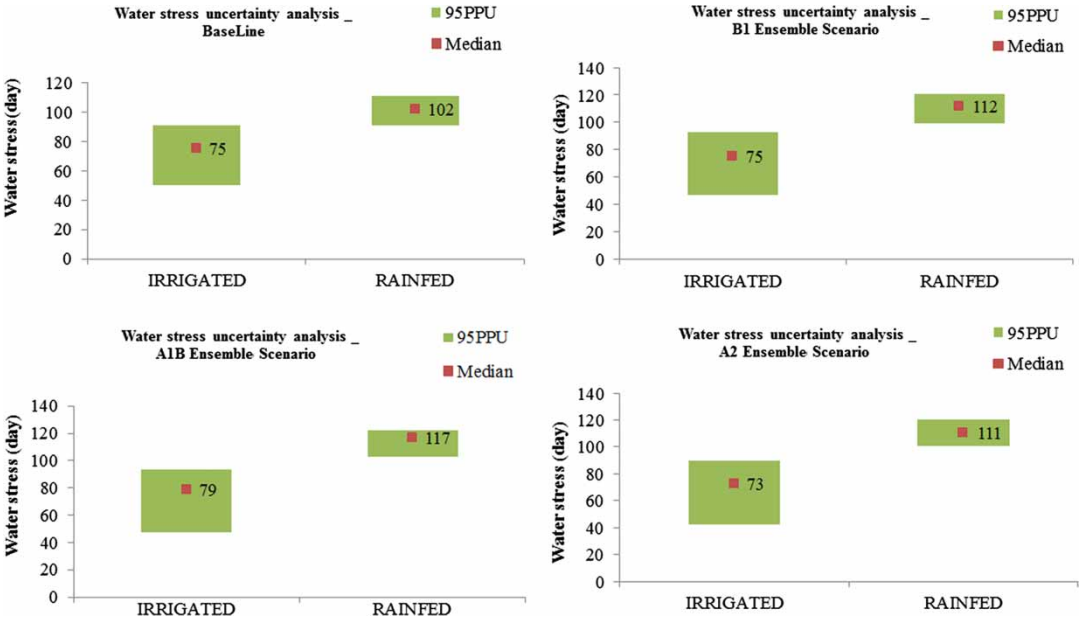

Figure 11 | Water stress uncertainty analysis in different scenarios both for irrigated and rain-fed areas.

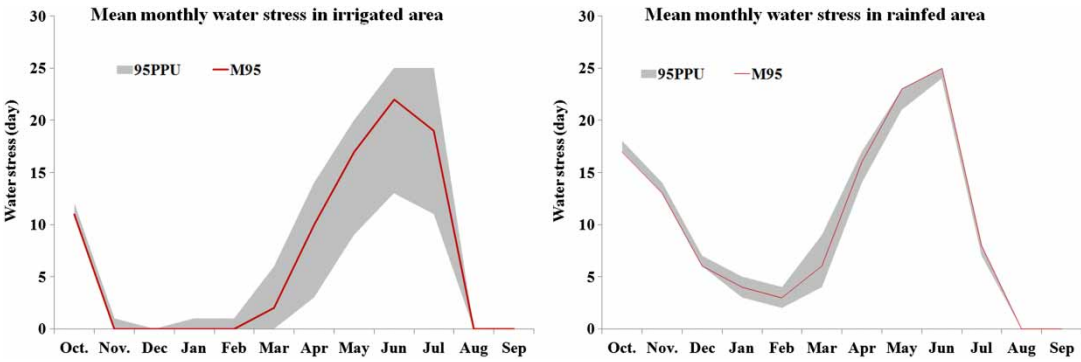

Figure 12 | Means monthly water stress in irrigated and rain-fed lands. 95 PPU, 95% prediction uncertainty; M95, median of iteration.

subsidence in the study area responds directly to groundwater resources. Owing to shortage of precipitation, groundwater is the main source of water resources for agriculture, industry and domestic purposes. In the west of the watershed due to the over-extraction of groundwater and sensitivity of the bedrock, land subsidences are occurring on a large scale.

The hydrograph of the aquifer was mapped based on piezometric wells data (Figure 13(a)). It revealed the trend of the water level falling about 20 m during the 21 years from 1988 to 2008. In other words, the water table is declining about 95 cm per year. The biggest decrease in the water level appeared in the west of the aquifer with approximately 3.5 m per year (Figure 13(b)). This huge fluctuation caused land degradations such as land subsidence and collapse and also salinization and other ecosystem deterioration. If the decline of the groundwater table continues to the same degree in the future, then the groundwater resources will be exhausted. To predict the water level of the aquifer in the future (2046–2065), we used the auto-regressive integrated moving average model (ARIMA). ARIMA is usually used to predict future points in the time-series course. The result shows a decrease of the water level up to 32 m in 2050 (Figure 14). The use of ARIMA for the prediction of

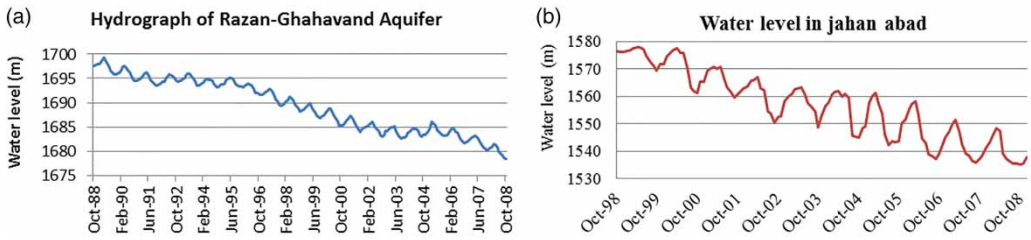

Figure 13 | Hydrographs of (a) Razan–Ghahavand aquifer and (b) degraded area in the western part of the basin (jahan abad).

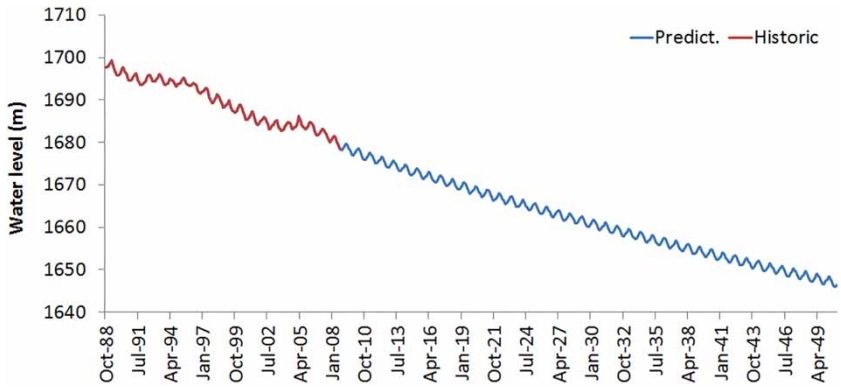

Figure 14 | Hydrograph of Razan–Ghahavand aquifer from historic period (1988) to 2050, predicted by ARIMA model.

groundwater levels is documented by other studies such as Changnon *et al.* (1988).

Table 2 shows the estimation of average annual recharge in the historic period (1998–2008) and the percentage difference between the future groundwater recharge (2046–2065) and the baseline groundwater recharge. The highest decrease (24%) is based on the A1B scenario and the lowest decline (8%) is found for scenario B1. The field observations show that most land subsidence is happening in HRU 515 and 571 in the west of the basin. Therefore, the groundwater recharge was estimated in these areas specifically. The results show an increase of recharge in those places up to 52% for scenario B1. The reason for a rising recharge is due to increasing precipitation in this part of the basin. Overall, we can conclude that for the future the whole basin is facing both declining groundwater table and decreasing groundwater recharge.

Table 2 | The rate of groundwater recharge in HRUs 515 and 571 (in the west of the basin) and the whole basin in base line and per cent difference calculated based on future (2046–2065) and historic (1998–2008) data

Scenario	HRU 571	HRU 515	Watershed
B1	52%	51%	−8%
A1B	44%	42%	−11%
A2	32%	39%	−24%
Bs	1.2 mm	1.3 mm	4.6 mm

CONCLUSION

This study investigated the ensemble climate change effect on hydrology, crop production and land degradation based on four GCMs in three emission scenarios. In addition, the impact of land use changes (urbanization) on runoff production was evaluated.

The Razan–Ghahavand basin is currently under high pressure due to growing water demand for drinking, agriculture and industrial purposes. The population has grown rapidly in the last 20 years. A future climate is likely to affect the water resources differently in the north and south of the basin. The spatial pattern of climate

change models shows that with increasing CO_2 the temperature is increased and it leads to more ET and less groundwater recharge. A similar result is reported by Bouraoui *et al.* (2004). We found that precipitation in the south and central part of the basin will decline while the northern and the western parts will face more precipitation. The increase of precipitation in the west is the reason for rising groundwater recharge in HRUs with land subsidence phenomena; therefore, the water table in this part of the basin will increase. In other words, with good water management in this area further land subsidence could be controlled. However, the rangelands in the southern part of the basin are under water stress which will continue even in the future due to the decrease in precipitation. However, we can conclude that the watershed will have less rain and high summer temperatures. Therefore, a sustainable strategy needs to be considered for future water resources development.

On the other hand, wheat is the representative crop in the basin and suffered from heat stress during the historical period. Therefore, with rising temperatures in the future, the production will increase especially in irrigated lands. Nevertheless, production in rain-fed areas will decrease due to water stress. The water stress in rain-fed areas is greater than in irrigated areas; however, the uncertainty in irrigated lands is due more to the unaccounted water use in the model due to lack of data. Hence, the increase of water use efficiency will be mandatory in future cropping systems for the sustainable use of water resources.

Urbanization growth has a significant effect on surface runoff. It is important to note that to develop a water resources management plan, certain LULC changes (e.g., urbanization) as well as associated flood patterns should be considered.

Finally, it is important to note that the predictions of hydrological components in the future were based on the use of the same soil parameters for baseline. In this study, the change of soil parameters was not considered in the future. Change of soil parameters may have an effect on soil water content as well as surface runoff in the basin. Therefore, further research on climate change assessment while considering soil parameter changes would raise confidence on the outcomes. The same limitations have already been discussed by Faramarzi *et al.* (2013).

We used a set of four GCMs in this study; however, considering the fact that the effect of other GCMs or even RCMs may have different outcomes, they should be studied in further research.

ACKNOWLEDGEMENTS

The authors would like to express their gratitude to Dr Karim C. Abbaspour and Dr Samira Akhavan for their helpful comments during the calibration processes of the SWAT model. We are grateful to the editor and anonymous reviewers whose valuable comments and suggestions improved the manuscript greatly.

REFERENCES

Abbaspour, K. C. 2007 *User Manual for SWAT-CUP, SWAT Calibration and Uncertainty Analysis Programs*. Swiss Federal Institute of Aquatic Science and Technology, EAWAG, Duebendorf, Switzerland, p. 93.

Abbaspour, K. C., Faramarzi, M., Ghasemi, S. S. & Yang, H. 2009 Assessing the impact of climate change on water resources in Iran. *Water Resour. Res.* **45** (10), 1–16.

Abrishamchi, A. & Tajrishi, M. 2005 Inter basin water transfer in Iran. In: *Water Conservation, Reuse, and Recycling. Proceedings of an Iranian American Workshop. National Academies Press*, Washington, DC, pp. 252–271.

Adams, R. M., Hurd, B. H., Lenhart, S. & Leary, N. 1998 Effects of global climate change on agriculture: an interpretative review. *Climate Res.* **11**, 19–30.

Ali, R., McFarlane, D., Varma, S., Dawes, W., Emelyanova, I., Hodgson, G. & Charles, S. 2012 Potential climate change impacts on groundwater resources of south-western Australia. *J. Hydrol.* **475**, 456–472.

Arnold, J. G., Srinivasan, R., Muttiah, R. S. & Williams, J. R. 1998 Large area hydrologic modeling and assessment – part 1: model development. *J. Am. Water Res. Assoc.* **34**, 73–89.

Baker, T. J. & Miller, S. N. 2013 Using the soil and water assessment tool (SWAT) to assess land use impact on water resources in an East African watershed. *J. Hydrol.* **486**, 100–111.

Bouraoui, F., Grizzetti, B., Granlund, K., Rekolainen, S. & Bidoglio, G. 2004 Impact of climate change on the water cycle and nutrient losses in a Finnish catchment. *Climatic Change* **66**, 109–126.

Changnon, S. A., Huff, F. A. & Hsu, C. F. 1988 Relations between precipitation and shallow groundwater in Illinois. *J. Climate* **1**, 1239–1250.

Eckhardt, K. & Ulbrich, U. 2003 Potential impacts of climate change on groundwater recharge and streamflow in a central European low mountain range. *J. Hydrol.* **284** (1–4), 244–252.

Faramarzi, M., Abbaspour, K. C., Ashraf Vaghefi, S., Farzaneh, M. R., Zehnder, A. J. B., Srinivasan, R. & Yang, H. 2013 Modeling impacts of climate change on freshwater availability in Africa. *J. Hydrol.* **480**, 85–101.

Fontaine, T. A., Klassen, J. F., Cruickshank, T. S. & Hotchkiss, R. H. 2001 Hydrological response to climate change in the Black Hills of South Dakota, USA. *Hydrol. Sci. J.* **46**, 27–40.

Gaiser, T., Judex, M., Igue, A. M., Paeth, H. & Hiepe, C. 2011 Future productivity of fallow systems in sub-Saharan Africa: is the effect of demographic pressure and fallow reduction more significant than climate change? *Agric. For. Meteorol.* **151**, 1120–1130.

Gosain, A. K., Rao, S. & Arora, A. 2011 Climate change impact assessment of water resources in India. *Curr. Sci. India* **101** (3), 356–371.

Hargreaves, G. & Samani, Z. A. 1985 Reference crop evapotranspiration from temperature. *Appl. Eng. Agric.* **1**, 96–99.

Hijioka, Y., Lin, E., Pereira, J. J., Corlett, R. T., Cui, X., Insarov, G. E., Lasco, R. D., Lindgren, E. & Surjan, A. 2014 Asia. In: *Climate Change 2014: Impacts, Adaptation, and Vulnerability. Part B: Regional Aspects. Contribution of Working Group II to the Fifth Assessment Report of the Intergovernmental Panel on Climate Change* (V. R. Barros, C. B. Field, D. J. Dokken, M. D. Mastrandrea, K. J. Mach, T. E. Bilir, M. Chatterjee, K. L. Ebi, Y. O. Estrada, R. C. Genova, B. Girma, E. S. Kissel, A. N. Levy, S. MacCracken, P. R. Mastrandrea & L. L. White, eds). Cambridge University Press, Cambridge, pp. 1327–1370.

IPCC 2007a The physical science basis – summary for policymakers. Contribution of WGI to the Fourth Assessment Report of the Intergovernmental Panel on Climate Change. http://www.ipcc.ch/ipccreports/ar4-wg1.htm.

IPCC 2007b *Climate Change 2007: The Scientific Basis*. IPCC Contribution of Working Group I to the Fourth Assessment Report of the Intergovernmental Panel on Climate Change. Cambridge University Press, Cambridge.

IPCC 2013 Climate Change 2013: The Physical Science Basis. In: *Contribution of Working Group I to the Fifth Assessment Report of the Intergovernmental Panel on Climate Change*, (T. F. Stocker, D. Qin, G.-K. Plattner, M. Tignor, S. K. Allen, J. Boschung, A. Nauels, Y. Xia, V. Bex & P. M. Midgley, eds). Cambridge University Press, Cambridge, UK and New York, USA, p. 1535.

IPCC 2014 Summary for policymakers. In: *Climate Change 2014: Impacts, Adaptation, and Vulnerability. Part A: Global and Sectoral Aspects. Contribution of Working Group II to the Fifth Assessment Report of the Intergovernmental Panel on Climate Change* (C. B. Field, V. R. Barros, D. J. Dokken, K. J. Mach, M. D. Mastrandrea, T. E. Bilir, M. Chatterjee, K. L. Ebi, Y. O. Estrada, R. C. Genova, B. Girma, E. S. Kissel, A. N. Levy, S. MacCracken, P. R. Mastrandrea & L. L. White, eds). Cambridge University Press, Cambridge, pp. 1–32.

Jin, X.-L., Xu, C.-Y., Zhang, Q. & Singh, V. P. 2010 Parameter and modeling uncertainty simulated by GLUE and a formal Bayesian method for a conceptual hydrological model. *J. Hydrol.* **383**, 147–155.

Jyrkama, M. I. & Sykes, J. F. 2006 *The Handbook of Groundwater Engineering: The Impact of Climate Change on Groundwater*. University of Waterloo, Ontario, Canada.

Kim, J., Choi, J., Choi, C. & Park, S. 2013 Impacts of changes in climate and land use/land cover under IPCC RCP scenarios on streamflow in the Hoeya River Basin, Korea. *Sci. Total Environ.* **452–453**, 181–195.

Kirshen, P. H. 2002 Potential impacts of global warming on groundwater in eastern *Massachusetts. J. Water Res.* **128**, 216–226.

Lawless, C. & Semenov, M. A. 2005 Assessing lead-time for predicting wheat growth using a crop simulation model. *Agr. For. Meteorol.* **135**, 302–313.

Li, L., Xia, J., Xu, C.-Y. & Singh, V. P. 2010 Evaluation of the subjective factors of the GLUE method and comparison with the formal Bayesian method in uncertainty assessment of hydrological models. *J Hydrol.* **390**, 210–221.

Li, L., Xu, C.-Y. & Engeland, K. 2013 Development and comparison in uncertainty assessment based Bayesian modularization method in hydrological modeling. *J. Hydrol.* **486**, 384–394.

Li, L. & Xu, C.-Y. 2014 The comparison of sensitivity analysis of hydrological uncertainty estimates by GLUE and Bayesian method under the impact of precipitation errors. *Stoch. Env. Res. Risk A.* **28** (3), 491–504.

Meadows, M. E. & Hoffman, T. M. 2003 Land degradation and climate change in South Africa. *Geogr. J.* **169** (2), 168–177.

Moriasi, D. N., Arnold, J. G., Van Liew, M. W., Bringer, R. L., Harmel, R. D. & Veith, T. L. 2007 Model evaluation guidelines for systematic quantification of accuracy in watershed simulations. *Am. Soc. Agric. Biol. Eng.* **50** (3), 885–900.

Neitsch, S. L., Arnold, J. G., Kiniry, J. R., Williams, J. R. & King, K. W. 2011 *Soil and water assessment* Tool. Theoretical documentation: Version 2000. TWRI TR-191. Texas Water Resources Institute, College Station, TX, USA.

Piao, S., Friedlingstein, P., Ciais, P., Peylin, P., Zhu, B. & Reichstein, M. 2009 Footprint of temperature changes in the temperate and boreal forest carbon balance. *Geophys. Res. Lett.* 36, L07404.

Rafiei Emam, A., Kappas, M. & Abbaspour, K. C. 2015a Simulation of water balance components in a watershed located in central drainage basin of Iran. In: *Remote Sensing of the Terrestrial Water Cycle, Geophysical Monograph 206* (V. Lakshmi, ed.). American Geophysical Union. Wiley & Sons, Hoboken, NJ, USA.

Rafiei Emam, A., Kappas, M., Akhavan, S., Hosseini, S. Z. & Abbaspour, K. C. 2015b Estimation of groundwater recharge and its relation with land degradation: case study of a semi-arid river basin in Iran. *Environ. Earth Sci.* doi:10.1007/s12665-015-4674-2.

Raleigh, C. & Urdal, H. 2007 Climate change, environmental degradation and armed conflict. *Polit. Geogr.* **26** (6), 674–694.

Ritchie, J. T. 1972 A model for predicting evaporation from a row crop with incomplete cover. *Water Resour. Res.* **8**, 1204–1213.

Rosenberg, N. J., Epstein, D. J., Wang, D., Vail, L., Srinivasan, R. & Arnold, J. G. 1999 Possible impacts of global warming on the hydrology of the Ogallala Aquifer Region. *Clim. Change* **42**, 677–692.

Santhi, C., Arnold, J. G., Williams, J. R., Dugas, W. A., Srinivasan, R. & Hauck, L. M. 2001 Validation of the SWAT model on a large river basin with point and nonpoint sources. *J. Am. Water Resour. Assoc.* **37** (5), 1169–1188.

Semenov, M. A. & Stratonovitch, P. 2010 Use of multi-model ensembles from global climate models for assessment of climate change impacts. *Clim. Res.* **41**, 1–14.

Singh, P. & Bengtsson, L. 2005 Impact of warmer climate onmelt and evaporation for the rainfed, snowfed and glacierfed basins in the Himalayan region. *J. Hydrol.* **300**, 140–154.

Statistical Center of Iran. 2011 Report of population rate. http://www.amar.org.ir/.

Sunyer, M. A., Madsen, H. & Ang, P. H. 2012 A comparison of different regional climate models and statistical downscaling methods for extreme rainfall estimation under climate change. *Atmos. Res.* **103**, 119–128.

Tong, S. T. Y., Sun, Y., Ranatunga, T., He, J. & Yang, Y. J. 2012 Predicting plausible impacts of sets of climate and land use change scenarios on water resources. *Appl. Geogr.* **32**, 477–489.

Tu, J. 2009 Combined impact climate and land use changes on streamflow and water quality in eastern Massachusetts, USA. *J. Hydrol.* **379**, 268–283.

Wand, S. J. E., Midgley, G. F., Jones, M. H. & Curtis, P. S. 1999 Responses of wild C4 and C3 grass (Poaceae) species to elevated atmospheric CO_2 concentration: a meta-analytic test of current theories and perceptions. *Glob. Change Biol.* **5**, 723–741.

Weng, Q. 2001 Modeling urban growth effects on surface runoff with the integration of remote sensing and GIS. *Environ. Manage.* **28**, 737–748.

Williams, J. R., Jones, C. A. & Dyke, P. T. 1984 A modeling approach to determining the relationship between erosion and soil productivity. *Trans. ASAE* **27** (1), 129–144.

World Wide Fund (WWF) 2010 Impacts of climate change on growth and yield of rice and wheat in the Upper Ganga Basin. http://awassets.wwfindia.org/downloads/.

Wu, Y., Liu, S. & Gallant, A. L. 2012 Predicting impacts of increased CO_2 and climate change on the water cycle and water quality in the semiarid James River Basin of the Midwestern USA. *Sci. Total Environ.* **430**, 150–160.

Xu, X. Y., Yang, H. B., Yang, D. W. & Ma, H. 2013 Assessing the impact of climate variability and human activities on annual runoff in the Luan River basin, China. *Hydrol. Res.* **44** (5), 940–952.

Young, C. A., Escobar-Arias, M. I., Fernandes, M., Joyce, B., Kiparsky, M. & Mount, J. F. 2009 Modeling the hydrology of climate change in California's Sierra Nevada for subwatershed scale adaptation. *J. Am. Water Resour. Assoc.* **45**, 1409–1423.

Zarghami, M., Abdi, A., Babaeian, I., Hassanzadeh, Y. & Kanani, R. 2011 Impacts of climate change on runoffs in East Azerbaijan, Iran. *Global Planet Change* **78**, 137–146.

Zektser, I. S. & Loaiciga, H. J. 1993 Groundwater fluxes in the global hydrologic cycle: past, present, and future. *J. Hydrol.* **144**, 405–442.

Zhan, C. S., Niu, C. W., Song, X. F. & Xu, C.-Y. 2013 The impacts of climate variability and human activities on streamflow in Bai River basin, northern China. *Hydrol. Res.* **44** (5), 875–885.

Zhou, F., Xu, Y. P., Chen, Y., Xu, C.-Y., Gao, Y. Q. & Du, J. K. 2013 Hydrological response to urbanization at different spatio-temporal scales simulated by coupling of CLUE-S and the SWAT model in the Yangtze River Delta region. *J. Hydrol.* **485**, 113–125.

First received 11 August 2014; accepted in revised form 25 December 2014. Available online 18 February 2015